Proceedings of ICAST2011:
22nd International Conference on Adaptive Structures and Technologies
October 10-12, 2011, Corfu, Greece

013

INFLUENCE OF ACTUATOR DYNAMICS ON THE LOAD REDUCTION POTENTIAL OF WIND TURBINES WITH DISTRIBUTED CONTROLLABLE RUBBER TRAILING EDGE FLAPS (CRTEF)

Thanasis K. Barlas, Risø-DTU **Helge A. Madsen, Risø-DTU**

ABSTRACT

The potential load reduction using Controllable Rubber Trailing Edge Flaps (CRTEF) on the 5MW NREL Reference Wind Turbine is investigated based on aeroservoelastic simulations using the HAWC2 code. A realistic case in terms of structural implementation is modeled, using one flap per blade located close to the tip, strain sensors at the blade root and inflow sensors at the flap position. The flap structural and aerodynamic characteristics are derived from numerical analysis and wind tunnel measurements on existing CRTEF prototypes developed at Risø – DTU. In HAWC2, the flap actuator dynamics are modeled as a first-order system and the unsteady aerodynamic effects of the flaps are modeled using the Gaunaa-Andersen dynamic stall model. Linear state-space models are obtained from HAWC2 using Subspace System Identification methods, for below-rated power and above-rated power operating points. Model Predictive Controllers (MPC) incorporating actuator constraints and using the strain and inflow signals on the blades are designed, based on the linear models. The effect of including the realistic actuator dynamics on the identified linear models and on the controller design is shown. The controllers are evaluated in non-linear HAWC2 simulations at various operating points. Focus is put on the influence of the flap actuator dynamics on the load reduction performance. The CRTEF implementation is shown to provide substantial blade root fatigue load reduction for normal power production load cases in turbulent wind. The actuator time constant is shown to considerably influence the predicted load reduction performance in an adverse manner. Conclusions are drawn regarding the effect of including the CRTEF actuator dynamics model in the full control design cycle (system identification, controller design and aeroservoelastic simulations) for load reduction predictions with active flaps.

1. INTRODUCTION

The size of wind turbines has been increasing rapidly over the past years. Rotors of more than 120m diameter are already commercially available, and prototypes with a rotor diameter of more than 160m are designed. Focusing on lowering the cost per kWh, new trends and technological improvements have been primary targets of research and development. One main focus is on developing new technologies capable of considerably reducing fatigue loads on wind turbines. New concepts for dynamic load reduction are focusing on a much faster and detailed load control, compared to existing individual blade pitch control, by utilizing active aerodynamic control devices distributed along the blade span. The concepts over the past 5 years have focused on the combination of actuators, aerodynamic surfaces such as flaps, sensors and controllers, which can provide dynamic load control. Such concepts are generally referred to as 'smart rotor control', a term used in rotorcraft research, and investigated for wind turbine applications over the past years, in terms of concept analysis [1, 2], aeroelastic analysis [3, 4, 5, 6, 7, 8, 10, 11], and small scale wind tunnel experiments [12, 13, 14, 15]. For a review of the state-of-the-art in the topic, the reader is referred to [16].

So far, results from numerical and experimental analysis mostly focusing on trailing edge flaps, have shown a considerable potential in fatigue load reduction. Moreover, the influence of flap type, placement and size, sensor type and location, and controller implementation, has been investigated in some of the above mentioned articles. Although, small scale blade and rotor experiments have utilized piezoelectric bender actuator concepts to provide

deformable trailing edge activation, such concepts are considered not directly up-scalable for modern large scale wind turbine blades, without any additional mechanical amplification parts. The lack of technology solutions for flap control for wind turbines initiated a development work at Risø - DTU in 2006 with the main objective to develop a robust and efficient flap system for implementation on MW scale turbines. This led to the design of the Controllable Rubber Trailing Edge Flap (CRTEF). The initial design studies led to the basic concept of a trailing edge flap manufactured in an elastic material such as e.g. rubber or plastic and with suitable reinforced voids that can be pressurized with a medium such as air or a liquid and in this way give the desired deflection of the flap. An important design issue identified from the beginning is the transient response of the actuator, due to the build-up of the pressure inside the system. Earlier studies have shown than additional time delays can considerably reduce the load alleviation potential [5].

The focus of this article is to investigate the influence of the CRTEF actuator characteristics on the predicted load reduction potential in the context of full wind turbine aeroservoelastic simulations with closed-loop active flap controls. This is carried out by including the aerodynamic and structural characteristics of the CRTEF design in the aeroservoelastic simulation environment, and also varying its dynamic response and studying its sensitivity to the predicted load reduction. Moreover, the influence of including knowledge of the actuator dynamics in the controller design process is explored, and its influence on the load reduction performance is analyzed. The aeroelastic code HAWC2, which includes unsteady aerodynamics modeling of trailing edge flaps, is used to generate system identification data, which is utilized in order to design Model Predictive Controllers (MPC) for the active flaps. The designed controllers are then evaluated in HAWC2 in terms of fatigue load reduction.

In section 2, the aeroelastic code HAWC2, used for the system identification data generation and the evaluation of designed controllers is briefly described. Details on the aerodynamics and dynamics characteristics of the simulated CRTEF implementation are provided. In section 3, the system identification algorithms application, and the identification results are presented. In section 4, the MPC controller design, including its optimization, tuning and incorporation of actuator constraints and inflow measurement signals, is described. In section 5, the designed controllers are evaluated using the aeroelastic code, at representative average wind speeds with standard normal power production load cases. Results in terms of fatigue load reduction are presented and analyzed, focusing on the influence of the actuator dynamics. Finally, in section 6, conclusions, discussion on the results, and future work are presented.

2. AEROESERVOELASTIC MODELING

2.1 Aeroelastic model and reference wind turbine

For generating system identification data in order to obtain linear models for controller design, and for evaluating the controller performance, the aeroelastic code HAWC2 is used, developed at Risø – DTU [17].

The structural part of HAWC2 is based on a multi-body formulation using the floating frame of reference approach, where wind turbine main structures are subdivided into a number of bodies where each body consists of an assembly of Timoshenko beam elements. Each body includes its own coordinate system, with calculation of internal inertia loads when this coordinate system is moved in space, so that large rotation and translation of the body motion is accounted for.

The aerodynamic forces are calculated using an unsteady Blade Element Momentum approach, including additional models for azimuthally dependent induction, dynamic inflow and tip losses. The aerodynamics of the flapped sections is taken into account by the Gaunaa-Andersen model [18], which is a type of Beddoes-Leishman dynamic stall model, and can be considered as a crossover between the work of Gaunaa [19] for the attached flow, and Hansen [20] for the separated flow region. The model calculates the unsteady sectional aerodynamic forces, as a function of the angle of attack and flap angle, accounting for the shed vorticity dynamics. The method is capable of simulating thin, variable geometry airfoils.

The wind input in HAWC2 includes models for wind shear, potential ‘tower shadow’ flow and the Mann turbulence model [21]. The aerodynamic drag of the tower and nacelle is also modeled.

The NREL 5MW Reference Wind Turbine (RWT) [22] is used for the simulations, as a representative modern multi-MW wind turbine model which has been used extensively for active controls studies. The main geometrical and operational properties of the reference wind turbine are shown in Table 1.

Table 1 NREL 5MW RWT baseline properties.

Wind regime	IEC Class 1B / Class 6 winds	-
Rotor Orientation	Clockwise rotation - Upwind	-
Control	Variable Speed / collective pitch	-
Cut in wind speed	4	m/s
Cut out wind speed	25	m/s
Rated power	5	MW
Number of blades	3	-
Rotor Diameter	126.0	m
Hub Diameter	3.0	m
Hub Height	90.0	m
Rated Rotor Speed	12.1	rpm
Rated Generator Speed	1,173.7	rpm
Gearbox Ratio	97.0	-
Shaft Tilt Angle	5.0	º
Rotor Precone Angle	-2.5	º

2.2 CRTEF

The basic design of the CRTEF concerns a flap made of flexible material, like rubber or plastic, with suitable reinforced voids that can be pressurized with a medium such as air or a liquid and in this way give the desired deflection of the flap. During the past 3 years at Risø - DTU, the CRTEF concept has been explored, in terms of numerical modeling and production of first prototypes. The COMSOL® [23] software package has been used for the Finite Element (FE) modeling of CRTEF configurations, exploring various void arrangements, and internal reinforcement structure concepts. Examples of produced designs are shown in Figure 1.

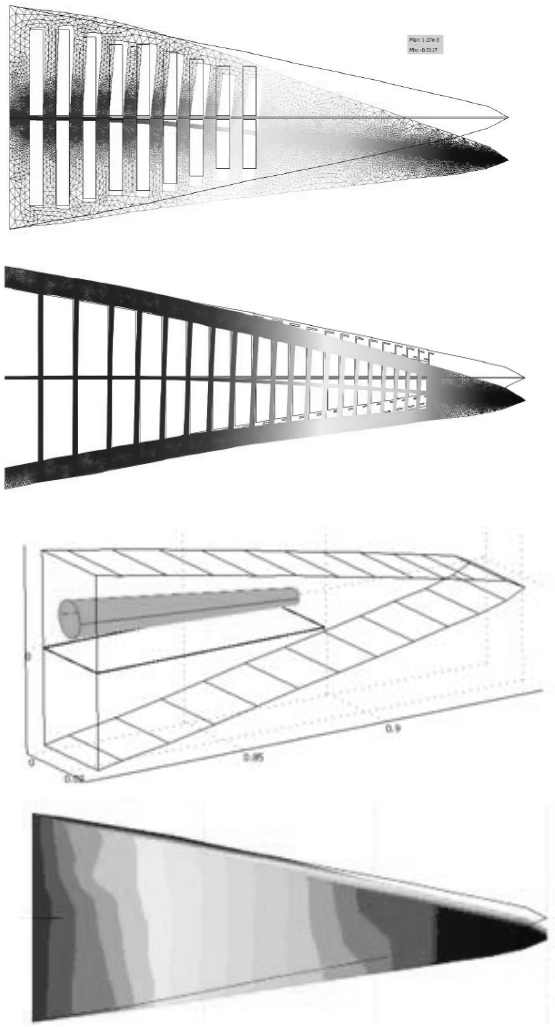

Figure 1. FE modeling of CRTEF configurations: (from upper to lower): span-wise voids 2D deformation, span-wise void with reinforcement 2D deformation, chord-wise voids 3D geometry, chord-wise voids 3D deformation.

A number of prototypes with a chord of 150 mm, based on the NACA0015 airfoil shape, have been manufactured and tested showing a maximum deflection of ± 12 mm for a pressure of ± 8 bar. Six of these prototypes were glued together and mounted on a 1.9 m long airfoil section model with a chord of 1 m (Figure 2). In the wind tunnel measurements the total ΔC_L for a maximum flap deflection was around ±0.2 [24].

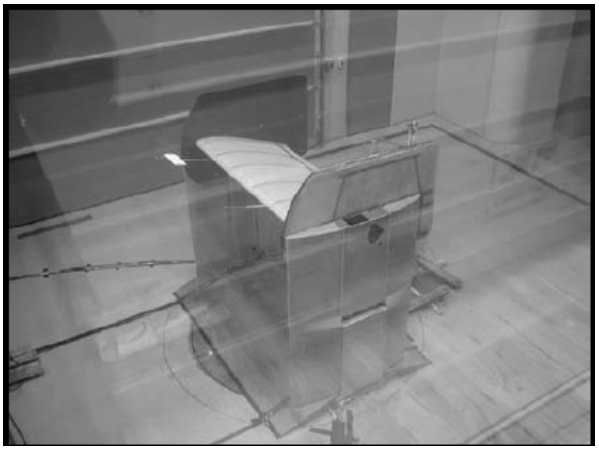

Figure 2. The wind tunnel model with a chord of 1m and span of 1.9 m equipped with a 15%c CRTEF.

The CRTEF so far has been developed to a stage where the functioning principle has been verified during lab and wind tunnel tests. In the context of a new development project, the CRTEF technology will be optimized up to a stage where it will be ready for installation as a prototype on a full scale MW turbine with the time frame of 2-3 years. Aspects of best possible polymer materials, production methods, and integration of the flap in the blade structural design are considered.

Based on the knowledge from the existing prototypes and wind tunnel tests, the characteristics of a CRTEF design implemented at the tip sections of the NREL 5MW RWT are derived. The set of inputs needed for aeroelastic simulations of wind turbines with specific active flaps in HAWC2, apart from controls implementation, consist of 2D aerodynamic properties, and, in the case of this article also, actuator dynamics characteristics. On the lack of specific design of structural integration of the CRTEF in the blade, it is assumed that the CRTEF does not influence the structural properties of the blade.

First, based on confidence on the prediction of aerodynamic properties of the existing CRTEF prototypes measured during wind tunnel tests (using 15%c CRTEF on NACA0015 airfoil), the numerical predictions are extended for the design of a 10%c CRTEF on the NACA64618 airfoil, which is used on the tip sections of the 5MW RWT. FE simulations have established the predicted deflection shape and achieved trailing edge angles, for designs based on the NACA64618 airfoil (Figure 3).

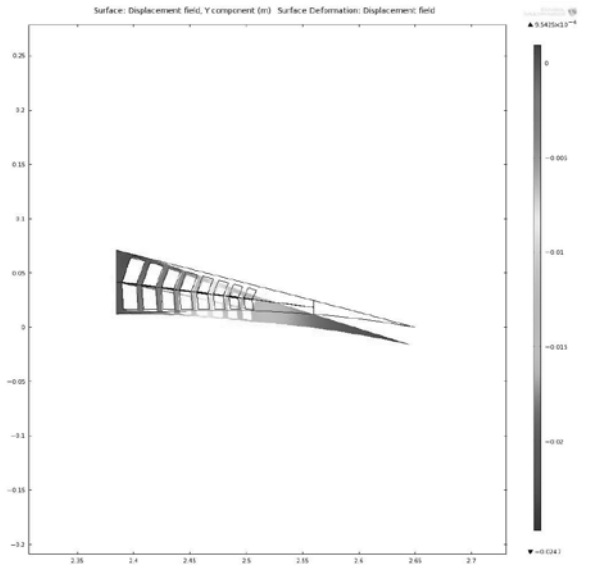

Figure 3. FE simulation result showing deflection of the 10%c CRTEF on the NACA64618.

The exact deflection shape of the CRTEF (Figure 4) is implemented on the NACA64618 geometry and predictions of steady aerodynamic coefficients are performed using 2D CFD computations. An average ΔC_l per flap angle of 0.04 is predicted. The polar for lift coefficient for a normal range of angles of attack α, is shown in Figure 5, including the effect of a ±5 deg. CRTEF deflection. The steady aerodynamic data is used by the Gaunaa-Andersen dynamic stall model to predict the unsteady aerodynamic response due to angle of attack and flap changes. The exact profile-specific constants for the indicial response functions, describing the circulatory part of the unsteady lift response in attached flow conditions, are used for the NACA64618 airfoil, obtained from CFD simulations.

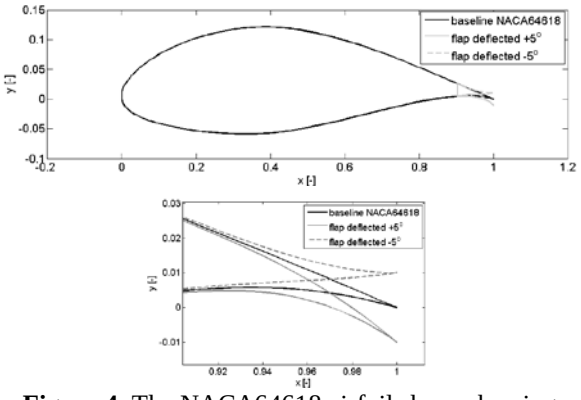

Figure 4. The NACA64618 airfoil shape showing deflection shape of CRTEF flap angles.

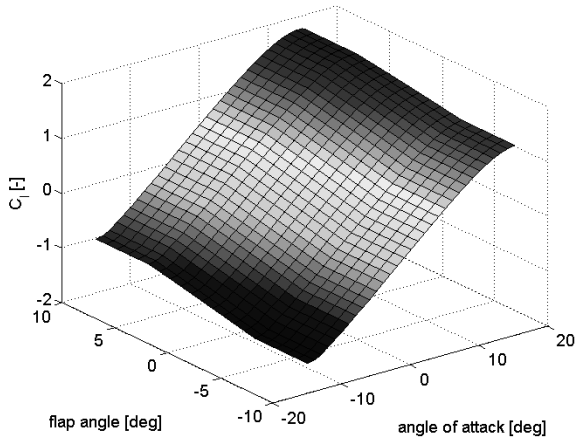

Figure 5. Steady C_l data for a range of angles of attack and flap angles for the NACA64618 showing the ΔC_l effect of the CRTEF.

The dynamic characteristics of the CRTEF have been derived from measurements on existing prototypes, and have been included in the HAWC2 simulations as an actuator model represented by a first order system with a certain time constant (Equation 1).

$$G(s) = \frac{1}{1 + s\tau}$$

(Equation 1)

The comparison of the response of the first order model with a time constant of 0.1s with the actual measurements is shown in Figure 6. The first order dynamics can describe the transient response of the actuator quite accurately.

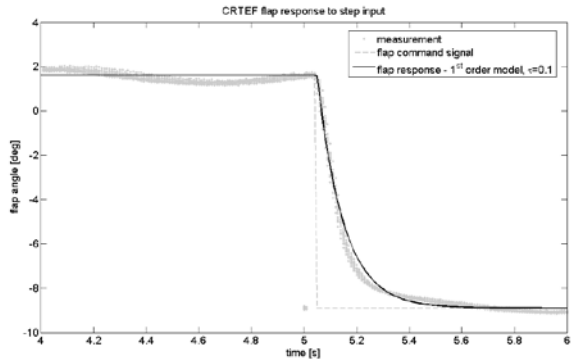

Figure 6. Measurement of the CRTEF response to a step in pressure and fitting of a first order linear model.

In the HAWC2 model, the 10%c CRTEF covers the 20% of the rotor radius, extending from 75%R to 95%R, as seen in Figure 7. A strain sensor is located at the blade root, which, in the simulations, provides a flap-wise blade root bending moment signal. An additional inflow sensor (e.g. Pitot tube) is located at the leading edge of the mid-flap position, which, in the simulations, provides an effective velocity at the corresponding section. The specific design is considered realistic in terms of structural implementation and simplicity. In [5,7,11] it is predicted that multiple flaps and distributed sensors can benefit the load reduction potential. The current design focuses on a simple and robust solution which could be implemented in current blade designs, without extensive retrofitting.

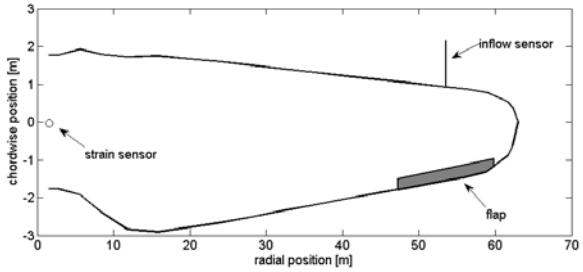

Figure 7. The blade planform showing size and location of flap and sensors.

2.3 Controllers

The active flap load controller is implemented at each blade utilizing both the strain and inflow signals and providing a flap deflection angle. The MPC controller design is described in section 4, using linear models obtained as described in section 3.

The baseline controllers of the 5MW RWT for rotor speed control and power regulation are used normally. These controllers consist firstly of a multi-region generator torque control, where the generator torque is given by a square function of the high speed shaft (HSS) rotational speed in below rated operation; whereas the generator torque is given as a ratio of rated power divided over the HSS speed in above rated operation. Linear slope regions are also included for the transient operation between the main regions. The HSS speed is filtered with a low-pass filter at 0.25 Hz in order to avoid aggressive response of the torque and pitch controller to high frequency vibrations at the shaft. In the above rated operation, the collective pitch angle is determined via a PI feedback control loop based on the filtered HSS speed. The gains are scheduled for every operating point, based on the pitch angle signal.

All controllers are implemented in Matlab® Simulink® (similarly to [11]) which is connected to HAWC2 via a TCP/IP connection interface.

3. SYSTEM IDENTIFICATION

3.1 Identification procedure

Modern control design techniques are usually based on a linear description of the system dynamics between inputs and outputs. In this work, these linear models are obtained using system identification with input/output data generated with HAWC2 at specific operating points. The utilized algorithm is the Predictor-Based Subspace Identification Toolbox (PBSID) [26] developed at the Delft Center for Systems and Control (DCSC) of Delft University of Technology (TUDelft). The algorithm, which has been used before in the context of wind turbine research, has the capability to identifying Linear Time Invariant (LTI) models from data generated from systems exhibiting periodic varying dynamics [27].

The identification `experiment´ is performed in HAWC2, by exciting the wind turbine dynamics during normal operation at a 10 minute simulation with a sample rate of 40 Hz, using a Gaussian Binary Noise (GBN) input signal for the flaps, and measuring the high-pass filtered (HPF) output blade root flap-wise moment. The input/output data for the case of normal operation at 7 m/s (with a turbulence intensity of 5%) is shown in Figure 8. The first input to the system is the command signal on the flaps, using the GBN sequence for the system identification, sampled at a lower sample rate compared to the simulation sample rate, in order focus the excitation on the lower frequency band. The second input is the measured HPF effective velocity at the mid-flap section, which is treated as a measured disturbance input, providing additional knowledge of inflow fluctuations. The output is the measured HPF blade root flap-wise moment. The reason for the high-pass filtering of the signals (which uses a corner frequency of 0.05 Hz) is that the control objective is to provide dynamic load control, without any pre-specified set-point. It should be noted that the HAWC2 model during the system identification `experiment´, is not idealized in any way, thus including various non-linearities and all deterministic and stochastic inflow elements.

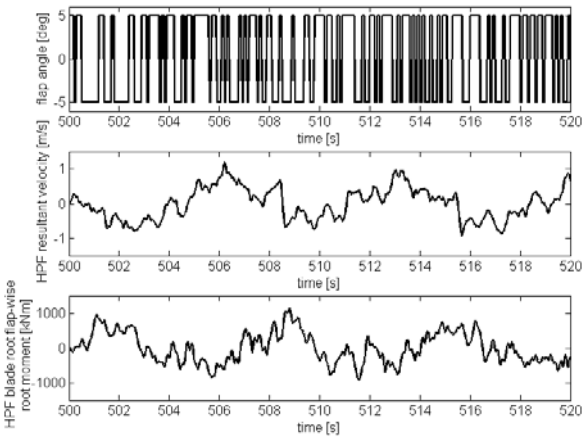

Figure 8. System identification input/output data for 7 m/s. From top to bottom: Gaussian Binary Noise (GBN) input signal on flap, high-pass-filtered (HPF) effective sectional velocity, high-pass-filtered (HPF) blade root flap-wise moment output.

Using the captured two input and one output signals, the subspace system identification algorithm is used in order to derive a consistent linear state-space model that describes the system between inputs and output (2x1) for the specific operating point.

The important variation for every identification `experiment´ performed in this work is the inclusion of the CRTEF actuator dynamics. So, for every operating point, two different linear models were identified; the one obtained from the HAWC2 data as described earlier, and the second additionally including the flap actuator dynamics as a first order system with a time constant of 0.1s.

3.3 Identification results

The accuracy of the models is determined on the basis of the variance-accounted-for (VAF) value (see [27]), which gives an indication of how well the measured output signals can be predicted using the model. The values obtained are in the order of 90%.

The obtained linear models are also simulated with the specified input signals and compared to the identification `experiment´ data from the non-linear simulations in HAWC2. A comparison of time-series output signals (HPF blade root flap-wise moment) is shown in Figure 9, for the case of 7 m/s.

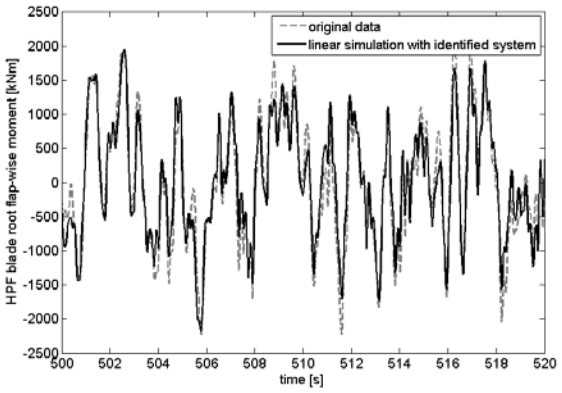

Figure 9. Comparison of simulated time series output of linear identified model with original non-linear data at 7 m/s.

As already mentioned, additional linear models, which include the flap actuator dynamics, were identified for the same operating points. The actuator dynamics transient response thus appears in the dynamics of these models. This is visible, for example, in a typical step response plot of the identified linear models with and without the actuator dynamics (Figure 10), where the HPF blade root flap-wise moment response of the system to a step input in the flap angle, including the actuator dynamics, shows an increased lag and reduced overshoot. Although the effect of the actuator lag in the dynamics in the linear model is not very pronounced, the influence of this on the controller design is investigated later on.

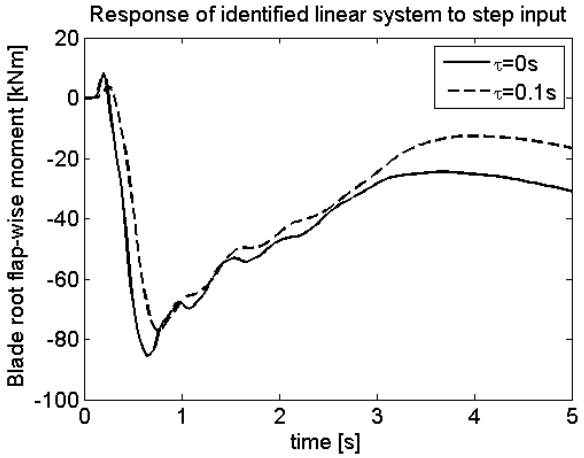

Figure 10. Comparison of identified linear models with and without flap actuator dynamics for 7m/s. Blade root flap-wise moment response to a step input in flap angle.

4. CONTROLLER DESIGN

4.1 MPC setup and optimization

A Model Predictive Control approach is used for the active flap load control, mainly because it incorporates an industry-based optimal type of control, including knowledge of actuator constraints and measured disturbances, and it generally does not require extensive retuning. The state-space models obtained from the aforementioned system identification method are directly used by the MPC to predict optimal sequences of control actions based on estimates of current states of the system and prediction of future outputs over some horizon.

The way the MPC controller is implemented in the current work is shown in Figure 11. The MPC control loop is implemented for each blade, and it uses the high-pass filtered blade root flap-wise moment signal in combination with a measurement of the effective velocity at the mid-flap section to calculate an optimal control move (flap angle) at every time step. One MPC control loop is implemented for each blade.

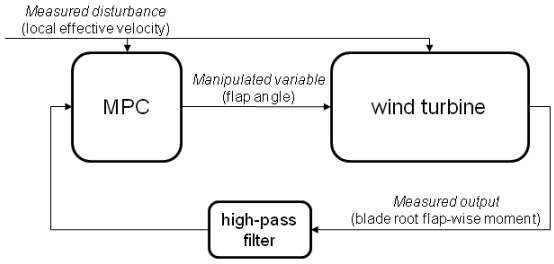

Figure 11. Layout of the MPC control system.

The state space model used by the MPC to predict the output of the system has the form shown in Equation 2

$$x(k+1) = Ax(k) + B_u u(k)\, B_v v(k) + B_d d(k)$$
$$y(k) = Cx(k) + D_u u(k) + D_d d(k)$$

(Equation 2)

where x is the state vector of the plant, u is the control variable, v is the measured disturbance, d is any unmeasured disturbance, and y is the system output. The A, B_u, B_v, C, D_u, and D_d matrices relate the control action, and the measured and unmeasured disturbances to the system states and its output. These are obtained from the system identification process. The unmeasured input and output disturbances are assumed to be zero mean unit covariance white noise.

The model predictive control action is obtained by minimizing the objective function J shown in Equation 3

$$J(k)=\sum_{i=1}^{P}\left(\left(\left(\hat{y}(k+i)-r(k+i)\right)w_y\right)^2+\left(u(k+i)w_u\right)^2+\left(\Delta u(k+i)w_{\Delta u}\right)^2\right)$$

(Equation 3)

where k is the current time instant, P is the prediction horizon (denoting number of sample times), $\hat{y}(k+i)$ is the predicted output at time instant i ,r is the set-point for the output, w_y is the weight for the output, u is the control action, w_u is the weight for the control action, Δ_u is the control action increment, $w_{\Delta u}$ is the weight for the control action increment. In our case we use a set-point r equal to 0, since we are interested in disturbance rejection.

Constraints are also added to the optimization problem, which account for control input saturation limits (Equation 4) and rate limits (Equation 5).

$$u_{min} \le u(k+i) \le u_{max}$$

(Equation 4)

$$\Delta u_{min} \le \Delta u(k+i) \le \Delta u_{max}$$

(Equation 5)

These limits on the flap angle and angle rate, specifically for our investigation, are taken as:

- $-5^o \le \delta \le 5^o$
- $-50^o/_s \le \dot{\delta} \le 50^o/_s$

corresponding to a conservative choice of characteristics achieved by the CRTEF.

Given that estimates of the current states are available, the output of the system can be predicted. The state estimates are provided by a Kalman filter, which combines measurements up to time instant k with the linear model of the system, to yield an optimal estimate of the current state of the system. The solution to the MPC optimization problem is the result of solving constrained quadratic program. In this way, optimal control actions are calculated over a finite horizon M called the control horizon (which is smaller than the prediction horizon P and again denotes number of sample times), and the solution on the first time instant is passed to the system. This procedure is updated at every time step, corresponding also to the time step of the HAWC2 simulation. The Matlab® Model Predictive Control Toolbox® is used in this case to solve the MPC problem.

4.2 MPC tuning

The MPC controllers are tuned offline for every operating point using the obtained linear models. The control parameters needed to be tuned are the prediction horizon P, the control horizon M, the output weight w_y, the input weight w_u and the input rate weight $w_{\Delta u}$. A convenient way to optimize the choice of the main controller parameters is to simulate the linear model in closed loop with the MPC, adding typical measured system output disturbances, taken from recorded sequences from HAWC2 simulations without flap controls [11]. Then the MPC parameters are optimized based on the achieved load reduction performance.

The MPC parameters are tuned for every operating point with a sequence of 100s of predicted HPF blade root flap-wise moment from HAWC2 simulations, for three different random turbulence seeds. Based on the optimal parameters, we see that that the values for the prediction horizon P and the control horizon M giving best load reduction results are on average around 26 and 4, respectively. For the case of the linear model in which the CRTEF actuator dynamics are included, we see optimal values of 30 and 4 for the P and M, respectively. This could indicate that for the case including the first order dynamics of the CRTEF actuator, a longer prediction horizon needs to be utilized due to the actuator lag.

5. RESULTS

5.1 Test cases and load reduction evaluation

The MPC controllers generated by tuning the main parameters with typical measured output from HAWC2 are then evaluated in normal power production simulations with HAWC2. A set of 600s simulations is performed for every operating point for three different turbulence random seeds. For every case the standard deviation of the blade root flap-wise moment is calculated. Moreover, the sequence of the blade root flap-wise moment values is rain-flow counted, where it is converted into moment amplitudes and corresponding number of cycles. The Miner's rule then is applied (using a material fatigue exponent of 10, representing a glass fiber composite structure) in order to yield a corresponding Damage Equivalent Load (DEL) for every case, which is used to compare results in terms of fatigue. The average values (over the three cases where different turbulence seeds used) for the achieved reduction in the standard deviation of the blade root flap-wise moment signal and in its DEL are calculated and compared to the cases with no MPC flap controls. The impact of the MPC flap control on the blade structural loads is thus evaluated by examining these achieved reductions.

This procedure is performed for a variety of controller and actuator dynamics scenarios, which are summarized in Table 2.

Table 2 Investigated scenarios regarding characteristics of actuator dynamics in linear models and HAWC2 simulations.

case	CRTEF actuator τ in linear model with which MPC is designed [s]	*CRTEF actuator* τ in HAWC2 where MPC is evaluated [s]
1	0	0
2	0	0.1
3	0	0.5
4	0	1
5	0.1	0.1
6	0.1	0.5
7	0.1	1

The case 1 represents an ideal scenario where the MPC controller is designed based on a linear model of the wind turbine which includes no actuator dynamics, and it is evaluated in HAWC2, also with no actuator dynamics. Cases 2, 3 and 4 represent scenarios where the MPC controller is designed based on a linear model of the wind turbine which includes no actuator dynamics, but it is evaluated in HAWC2, including actuator dynamics with a realistic time constant τ for a normal CRTEF design (case 2), and with exaggerated time constants representing a slower actuation system (cases 3 and 4). Cases 5, 6 and 7 represent scenarios where the MPC controller is designed based on a linear model of the wind turbine which includes normal CRTEF actuator dynamics (τ=0.1s), and it is evaluated in HAWC2, including actuator dynamics with a realistic time constant τ for a normal CRTEF design (case 5), and with exaggerated time constants representing a slower actuation system (or possibly actuator degradation) (cases 6 and 7).

5.2 Load reduction potential and influence of actuator dynamics

The application of the designed MPC controllers in HAWC2 simulations reveals the achieved dynamic load reduction. A representative time series of inflow conditions, aeroelastic response and control signals is shown in Figure 12, for the case 1 scenario at below rated operation with 7 m/s.

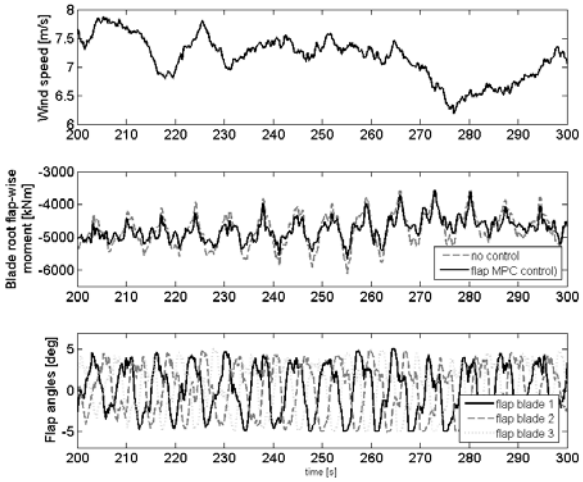

Figure 12. Time series of wind speed, blade root flap-wise moment (with and without MPC flaps control) and flap angles for the case 1 scenario at 7m/s.

The achieved load reduction, as seen in the controlled signal of the blade root flap-wise moment compared to the uncontrolled one, is considerable. The utilized flap control angles remain within the constraint levels. A dominant 1P signal is seen in both the blade root flap-wise moment signal and the flap command signals. This more pronounced due to the low turbulence intensity in this case. For this case 1 scenario, a reduction of 24.6 % in the standard deviation of the blade root flap-wise moment signal is calculated, compared to the case with no flap controls.

The evaluation of the load reduction is performed for each of the predefined scenarios in 600s simulations, where the reduction in the standard deviation of the blade root flap-wise moment signals and in its damage equivalent load are calculated. The results for every case, averaged over the three different turbulence seeds, are shown in Table 3. The description of each case, in terms of actuator dynamic parameters, is shown in Table 2.

Table 3 Results for every case and two average wind speeds, regarding average reduction in the Standard Deviation (SD) of the blade root flap-wise moment and its Damage Equivalent Load (DEL).

case	% reduction in SD of blade root flap-wise moment		% reduction in DEL of blade root flap-wise moment	
	7 m/s	15 m/s	7 m/s	15 m/s
1	24.60	23.86	20.13	16.99
2	22.09	22.85	15.64	14.61
3	20.66	17.61	12.48	11.12
4	15.91	10.74	11.12	7.57
5	23.60	23.27	18.97	16.44
6	22.69	17.99	16.08	12.92
7	17.56	11.33	13.41	8.04

It is seen that the achieved load reduction in the `ideal´ case 1, where the flap actuator dynamics are not taken into account, is considerable, and in the same order as previously reported predictions [11]. Introducing a first order response corresponding to the CRTEF flap actuator, results in less load reduction (case 2). Further increase in the lag of the actuator (cases 3 and 4), considerably reduces the achieved load alleviation. When the controller is designed based on linear models which include the CRTEF flap actuator dynamics, the achieved load alleviation is increased when actuator dynamics are present, compared to the case where the controller is designed based on a model without actuator dynamics.

The trend in the predicted load reduction in relation to the applied lag in the flap actuator can be seen in Figure 13 for an average wind speed of 7m/s, and in Figure 14 for an average wind speed of 15m/s.

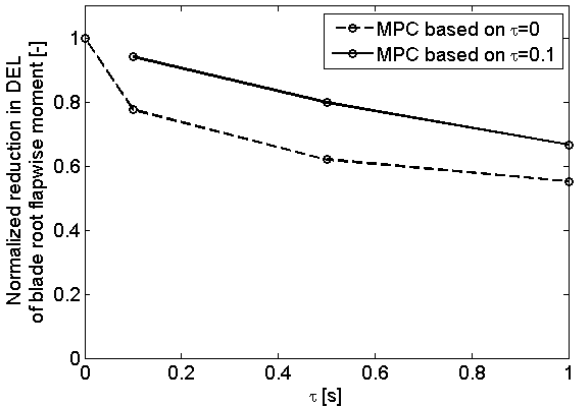

Figure 13. Normalized reduction in DEL of blade root flap-wise moment for various flap actuator time constants and two MPC designs at average wind speed of 7m/s.

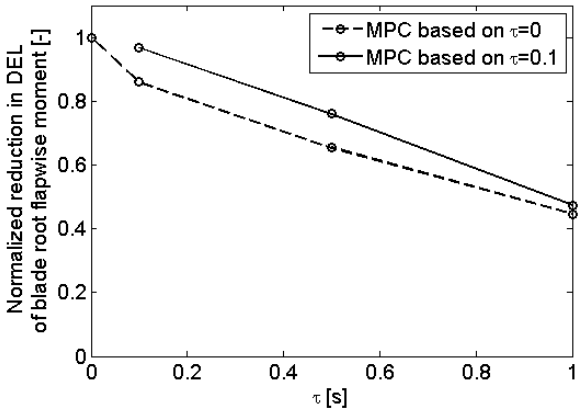

Figure 14. Normalized reduction in DEL of blade root flap-wise moment for various flap actuator time constants and two MPC designs at average wind speed of 15m/s.

6. CONCLUSIONS

The present research work has focused on the numerical prediction of the potential load reduction using Controllable Rubber Trailing Edge Flaps (CRTEF) on multi-MW wind turbines, by utilizing system identification procedures, MPC controller optimization, and aeroservoelastic simulations with the HAWC2 code. Optimal controllers using strain and inflow signals are designed and evaluated, with the focus on influence of the flap actuator dynamics. It is shown that the first order flap actuator dynamics influence both the controller design and the achieved load alleviation levels. Increased actuator lag considerably reduces the predicted fatigue load reduction. In the case where the actuator dynamics are taken into account in the controller design, the losses in

the achieved load reduction due to the actuator lag are less pronounced.

Future work on the subject will focus on the optimization of the CRTEF design, the connection to the blade structural design, and the efficient combination of the active flap load reduction controllers with the power regulation controllers.

ACKNOWLEDGMENTS

This research work is carried in the context of the project ` Industrial adaptation of a flap system for wind turbines´, funded by the Technology Development and Demonstration program EUDP of the Ministry for Climate and Energy in Denmark.

REFERENCES

1. Barlas, T.K., and van Kuik, GAM., 2007, State of the art and prospectives of smart rotor control for wind turbines, *J. Phys.: Conf. Ser.* 75 012080.
2. Johnson, S.J., Baker, J.P., van Dam, C.P., and Berg, D., 2010, An overview of active load control techniques for wind turbines with an emphasis on microtabs, *Wind Energy*; 13(2-3), 239-253.
3. Riziotis, V.A., and Voutsinas, S.G., 2008, Aero-elastic modelling of the active flap concept for load control, *Proceedings of the EWEC 2008*, Brussels, Belgium.
4. Andersen, P.B., Henriksen, L.C., Gaunaa, M., Bak, C., and Buhl, T., 2008, Integrating deformable trailing edge geometry in modern mega-watt wind turbine controllers, *Proceedings of the EWEC 2008*, Brussels, Belgium.
5. Andersen, P.B., Henriksen, L., Gaunaa, M., Bak, C., and Buhl, T., 2010, Deformable trailing edge flaps for modern megawatt wind turbine controllers using strain gauge sensors, *Wind Energy*; 13(2-3), 193-206.
6. Lackner, M.A., and van Kuik, G.A.M., 2010, A comparison of smart rotor control approaches using trailing edge flaps and individual pitch control, *Wind Energy*; 13(2-3), 117-134.
7. Barlas, T.K., and van Kuik, G.A.M., 2009, Aeroelastic Modelling and Comparison of Advanced Active Flap Control Concepts for Load Reduction on the Upwind 5MW Wind Turbine, *Proceedings of the EWEC 2009*, Marseille, France.
8. Resor, B., Wilson, D., Berg, D., Berg, J., Barlas, T., van Wingerden, J.-W., and van Kuik, G.A.M., 2010, Impact of higher fidelity models on simulation of active aerodynamic load control for fatigue damage reduction, *Proceedings of the 48th AIAA/ASME*, Orlando, FL, U.S.A.
9. Wilson, D., Resor, B., Berg, D., Berg, J., Barlas, T., and van Kuik, G.A.M., 2010, Active aerodynamic distributed flap control design procedure for load reduction, *Proceedings of the 48th AIAA/ASME*, Orlando, FL, U.S.A.
10. Berg, D., Wilson, D., Resor, B., Berg, J., Barlas, T., Crowther, A., and Halse, C., 2010, System ID modern control algorithms for active aerodynamic load control and impact on gearbox loading, *Proceedings of the Conference on the Science of Making Torque from Wind*, Heraklion, Greece.
11. Barlas, T.K, van der Veen, G.J., and van Kuik, G.A.M., 2011, Model Predictive Control for wind turbines with distributed active flaps: Incorporating inflow signals and actuator constraints. *Wind Energy*, to appear.
12. Bak, C., Gaunaa, M., Andersen, P.B., Buhl, T., Hansen, P., and Clemmensen, K., 2010, Wind tunnel test on airfoil Risø-B1-18with an Active Trailing Edge Flap, *Wind Energy*; 13(2-3), 207-219.
13. vanWingerden, .J-W., Hulskamp, A.W., Barlas, T., Marrant, B., van Kuik, G.A.M., Molenaar, D.-P., and Verhaegen, M., 2008, On the Proof of Concept of a Smart Wind Turbine Rotor Blade for Load Alleviation, *Wind Energy*; 11(3), 265-280.
14. Hulskamp, A.W., van Wingerden, J.-W., Barlas, T., Champliaud, H., van Kuik, G.A.M., Bersee, H.E.N., and Verhaegen, M., 2011, Design of a scaled wind turbine with a smart rotor for dynamic load control experiments, *Wind Energy*; 14(3), 339-354.
15. van Wingerden, J.-W., Hulskamp, T., Barlas, T., Houtzager, I., and Verhaegen, M., 2010, Two-degree-of-freedom active vibration control of a prototyped ”smart” rotor, *Journal of IEEE transactions on control system technology*; 19(2), 284-296.
16. Barlas, T.K., and van Kuik, G.A.M., 2010, Review of state of the art in smart rotor control research for wind turbines, *Prog Aerospace Sci* 46 (2010), 1-27.
17. Larsen, T.J., and Hansen, A.M., 2006, Influence of Blade Pitch Loads by Large Blade Deflections and Pitch Actuator Dynamics Using the New Aeroelastic Code HAWC2, *Proceedings of the EWEC 2006*, Athens, Greece.
18. Andersen, P.B., Gaunaa, M., Bak, C., and Hansen, M.H., 2010, A dynamic stall model for airfoils with variable trailing edges, *Wind Energy*, 12, 734-751.
19. Gaunaa, M., 2010, Unsteady two-dimensional potential-flow model for thin variable geometry airfoils, *Wind Energy*, 13, 167-192.
20. Hansen, M.H., Gaunaa M, and Madsen H.A., 2004, A Beddoes– Leishman type dynamic stall model in state-space and indicial formulations, *Technical Report*, Risø-R1354(EN).
21. Mann, J., 1998, Wind field simulation, *Prob. Engng. Mech.*, 13(4), 269-282.
22. Jonkman, J., Butterfield, S., Musial, W., and Scott, G., 2009, Definition of a 5-MW Reference Wind Turbine for Offshore System Development, *Technical Report*, National Renewable Energy Laboratory, NREL/TP- 500-38060.
23. COMSOL Multiphysics www.comsol.com/products/multiphysics/.
24. Madsen, H.A., Andersen, P.B., Andersen, T.L., Bak, C., and Buhl, T., 2010, The potentials of the controllable rubber trailing edge flap, *Proceedings of the EWEC 2010*, Warsaw, Poland.

*25.*Drela, M., 1989, XFOIL: An Analysis and Design System for Low Reynolds Number Airfoils, *Proceedings of the Conference on Low Reynolds Number Airfoil Aerodynamics*, Notre Dame, IN, U.S.A.

*26.*Houtzager, I., van Wingerden, J.-W., Verhaegen, M., 2010, Predictor-based Subspace Identification Toolbox Version0.4", http://www.dcsc.tudelft.nl/~datadriven/pbsid/.

*27.*van Wingerden, J.-W., Houtzager, I., Felici,F., Verhaegen, M., 2009, Closed-loop identification of the time-varying dynamics of variable-speed wind turbines, *International Journal of robust and nonlinear control special issue on Wind turbines: New challenges and advanced control solutions*, 19(1), 4-21.